Electrochimica Acta 556 (2026) 148448

Contents lists available at ScienceDirect

Electrochimica Acta

journal homepage: www.journals.elsevier.com/electrochimica-acta

Sustainable stencil-printed unmodified graphite–rosin electrode for electrochemical detection of ketamine in forensic samples

Jamilson P. Campos [a], Larissa M.A. Melo [a], Danielly S. Rocha [a], Daniel Júnior A. dos Santos [a], Maurício M.L. Pereira [a], Wallans T.P. dos Santos [b], Luciano C. Arantes [c,d], Wendell K.T. Coltro [a,e,*]

[a] Instituto de Química, Universidade Federal de Goiás, Campus Samambaia, 74690-900, Goiânia, Goiás, Brazil
[b] Departamento de Farmácia, Universidade Federal dos Vales do Jequitinhonha e Mucuri, Campus JK – Diamantina/MG, Brazil
[c] Forensic Chemistry and Physics Laboratory, Criminalistics Institute, Civil Police of the Federal District, 70610-907, Brasília, Distrito Federal, Brazil
[d] Instituto Nacional de Ciência e Tecnologia sobre Substâncias Psicoativas, Belo Horizonte, 31270-901, MG, Brazil
[e] National Institute of Science and Technology in Bioanalytics Lauro Kubota (INCTBio-LK), Instituto de Química, Universidade Estadual de Campinas (Unicamp), PO Box 6154, 13083-970, Campinas, SP, Brazil

ARTICLE INFO

Keywords:
Sustainable materials
Crime-facilitating substance
Biological samples
Illicit drugs
Forensics
Point-of-care (POC) technologies

ABSTRACT

Ketamine (KET) is a clinically used anesthetic with a high potential for abuse. Recreational and improper use of this substance pose significant health risks, including psychological, cardiovascular, neurotoxic, and dependency-related effects. However, there is currently no official and reliable method for its preliminary detection. Therefore, the development of rapid, selective, and simple analytical methods for KET detection is of great interest in both clinical and forensic contexts. In this study, we present an unprecedented application of rosin – a natural, eco-friendly resin derived from *Pinus* species – as a green binding additive in graphite-based conductive formulations for the fabrication of stencil-printed electrodes (graphite-pine rosin composite stencil electrode, GPC-SE). The GPC-SE fabrication process was optimized, and ideal conditions for reversibility and performance were established with a composition of 45% rosin, 55% graphite, and 5 mL of solvent. The resulting sensor was characterized by Raman spectroscopy, scanning electron microscopy, and electrochemical techniques. The GPC-SE combined with square-wave voltammetry exhibited wide linear range (50–500 μmol L^{-1}) in Britton-Robinson buffer solution (pH 8, 50 mmol L^{-1}), high sensitivity and low limits of detection (3.3 μmol L^{-1}) and quantification (10.1 μmol L^{-1}). The developed GPC-SE provided satisfactory reproducibility (RSDs <1.0% for E_P and <7% for I_P) and accuracy based on addition-recovery experiments on seized samples, beverages, and spiked biological samples. These findings demonstrate the applicability of the method in both forensic and clinical scenarios as rapid, reliable, and sustainable strategy for on-site identification of KET.

1. Introduction

Ketamine (KET) is a dissociative anesthetic that has been used clinically since the 1960s; however, its recreational use has increased due to its dissociative and hallucinogenic effects. Chronic consumption is associated with urinary, gastrointestinal, and neuropsychiatric complications [1]. Moreover, KET may induce psychological dependence and is occasionally employed as a crime-facilitating substance due to its sedative and amnesic properties [2]. Its growing availability, both legal and illicit, contributes to recreational use and poses public health and safety concerns in multiple countries [3].

Due to its abuse potential, KET is classified by the United States Drug Enforcement Administration as a Schedule III controlled substance, subject to federal regulation [4]. In parallel, KET can also be recognized as a New Psychoactive Substance (NPS) due to its emerging recreational use outside the traditional medical context, being monitored internationally by both the illicit market and public health authorities [4]. Furthermore, KET has frequently been identified as an adulterant in ecstasy, cocaine, and methamphetamine samples [5]. The detection of NPS such as KET outside clinical settings represents a significant challenge. The United Nations Office on Drugs and Crime (UNODC) recommends a two-step approach for NPS detection: (1) preliminary rapid

* Corresponding author.
E-mail address: wendell@ufg.br (W.K.T. Coltro).

https://doi.org/10.1016/j.electacta.2026.148448
Received 9 November 2025; Received in revised form 1 February 2026; Accepted 12 February 2026
Available online 12 February 2026

screening using colorimetric tests or immunochromatographic strips (dipsticks) for detection in urine or blood, allowing initial field identification; and (2) confirmatory testing using conventional techniques, including gas or liquid chromatography coupled with mass spectrometry, to validate results [6]. However, these screening methods lack selectivity and may produce false-positive or false-negative outcomes, which substantially limit the rapid and selective detection of NPS.

Given these challenges, the development of new portable and accessible analytical methods for the preliminary detection of KET is of significant interest in forensic applications. Electrochemical techniques have increasingly gained prominence for preliminary drug analysis [7] offering rapidity, high sensitivity, selectivity, and ease of use [8]. Various types of electrodes can be employed, including boron-doped diamond electrodes [9–11], glassy carbon electrodes [12], carbon-based electrodes produced by 3D printing [13–17], and screen-printed or stencil-printed electrodes [18,19]. The latter are particularly advantageous due to their low sample volume requirements (μL), portability, and simplicity, and they have been widely applied in the detection of diverse drug classes, such as amphetamines [20], phenylethylamines [21,22], synthetic cathinones [9,23,24], and KET [25,26].

In this study, we report the development of a lab-made electrode produced by stencil printing with carbon ink and rosin (graphite–pine rosin composite stencil electrode, referred to as GPC-SE) for in-situ KET detection. Rosin is a natural and environmentally sustainable resin that has been previously reported as an efficient component in the formulation of conductive inks [27]. It is a hard, yellowish solid obtained from the distillation of oleoresin extracted from trees of the *Pinus* genus. Its chemical composition is predominantly based on resin acids, including abietic, palustric, levopimaric, dehydroabietic, and neoabietic acids, along with a fraction of neutral compounds (approximately 5–10 %) belonging to the pimaric class, which confers broad industrial applicability [27]. However, because rosin is mainly composed of resin acids (e.g., abietic-type acids), it may undergo oxidative degradation under repeated potential cycling, potentially compromising the long-term reproducibility and durability of the electrode response [27]. The proposed GPC-SE sensors were investigated for the detection of KET in samples of forensic relevance, including seized materials and beverages, as well as in biological matrices of clinical interest, based on square-wave voltammetry (SWV) measurements. The main advances of this work lie in the use of a rosin-based conductive ink that enables simple fabrication, low material cost, mechanical robustness, and potential scalability of the electrode platform. These features, combined with compatibility with portable electrochemical instrumentation, position the proposed approach as a practical and sustainable alternative for in situ forensic screening applications.

2. Experimental section

2.1. Chemicals, materials and samples

KET analytical standard was provided by the United Nations Office on Drugs and Crime (UNODC) in powder form and diluted in 1 mL of HPLC-grade methanol (Sigma-Aldrich, St. Louis, MO, EUA) to obtain a stock solution of 10^{-2} mol L^{-1}. Real samples in tablet form were supplied by the Civil Police of the Federal District (PCDF) - Brazil. These samples underwent an extraction procedure at the PCDF, in which they were weighed, macerated, and diluted in 1 mL of HPLC-grade methanol. The resulting solutions were subsequently diluted in a suitable supporting electrolyte for electrochemical analysis and/or in an appropriate solvent for confirmatory methods. Synthetic biological matrices, including artificial saliva, synthetic urine, and artificial vitreous humor, were prepared as previously described elsewhere [28–30] while human serum was obtained from Sigma-Aldrich (St. Louis, MO, USA).

Potential interferents in KET detection, including 3,4-methylenodioxymethamphetamine (MDMA), procaine, lidocaine, cocaine, mephedrone, methadone, and morphine, as well as a commonly found adulterant (paracetamol) [31], were evaluated using the proposed method at concentrations of 10^{-2} molL^{-1}. All reagents were of analytical grade, with drug standards obtained from UNODC and paracetamol from Sigma-Aldrich (St. Louis, MO, USA).

For electrochemical characterization, ferro-/ferricyanide ($[Fe(CN)_6]^{4-/3-}$) and hexaammineruthenium ($[Ru(NH_3)_6]^{2+/3+}$) solutions were prepared at 1.0 mmol L^{-1} in 0.1 mol L^{-1} KCl. A 0.05 mol L^{-1} Britton–Robinson (BR) buffer solution was prepared by mixing boric, phosphoric, and acetic acids (purities > 99.9 %), and the pH was adjusted between 2–12 using 1.0 mol L^{-1} NaOH. Additional supporting electrolytes were also evaluated including borate and phosphate buffers (0.1 mol L^{-1}, pH 8.0), as well as BR buffer solutions at different concentrations. Acetic acid was used for electrochemical cleaning of the working electrode (WE) of the GPC-SE. Ultrapure water (18.2 MΩ cm) obtained from a Millipore Direct–Q®3 purification system was used to prepare all solutions.

Graphite powder, silver ink, EVA-coated polyester substrate, and vinyl adhesive were from Sigma-Aldrich (St. Louis, MO, USA), Joint Metal Commercial LTDA (São Paulo, Brazil), and purchased locally, respectively.

2.2. Production of conductive carbon-rosin ink

The conductive ink was prepared by varying the proportions of the conductive material (graphite) and the binder (rosin), as well as the volume of the solvent (acetone). Different graphite–rosin compositions were calculated and weighed at ratios of 40:60% (1.20 g of graphite, 1.80 g of rosin, and 5 mL of acetone), 45:55% (1.35 g of graphite, 1.65 g of rosin, and 5 mL of acetone), 50:50% (1.50 g of graphite, 1.50 g of rosin, and 5 mL of acetone), and 55:45% (1.65 g of graphite, 1.35 g of rosin, and 5 mL of acetone). The resulting mixtures were homogenized under magnetic stirring for 15–20 min to optimize the parameters influencing the chemical composition and consistency of the carbon-based ink.

2.3. Construction of GPC-SE

The GPC-SE was fabricated following the procedure described elsewhere [32], with specific adaptations. Two layers of vinyl adhesive (8 cm × 11 cm) were affixed onto a polyester substrate (80 mm × 110 mm × 250 μm). The integrated electrode layout was designed using Silhouette Studio® software, comprising a working electrode (WE; $\phi = 4$ mm), a reference electrode (RE), and an auxiliary electrode (AE). The electrode patterns were cut into the vinyl adhesive using a Silhouette cutting plotter (Belo Horizonte, MG, Brazil).

Subsequently, the adhesive layers containing the electrode stencil were mechanically removed from the polyester substrate using tweezers, as illustrated in Scheme 1a. The previously prepared conductive carbon ink was then deposited, following the methodology depicted in Scheme 1b, onto the regions corresponding to the working electrode (WE), auxiliary electrode (AE), and electrical connections.

The optimized carbon ink was spread over the stencil pattern using a spatula and allowed to dry at room temperature for 40 min. After complete solvent evaporation and ink curing, the remaining adhesive layers were mechanically removed using tweezers, fully releasing the polyester substrate from the vinyl mold and ensuring the structural integrity of the printed electrode layer, as shown in Scheme 1b.

Thereafter, a hydrophobic barrier was applied to define the sample deposition area on the GPC-SE. For this purpose, a commercial nail polish (Colorama Cremoso Leite de Coco, 8 mL), mainly composed of nitrocellulose dissolved in volatile solvents, was used to promote the rapid formation of a homogeneous film. Finally, the reference electrode (RE) was fabricated using commercial silver ink.

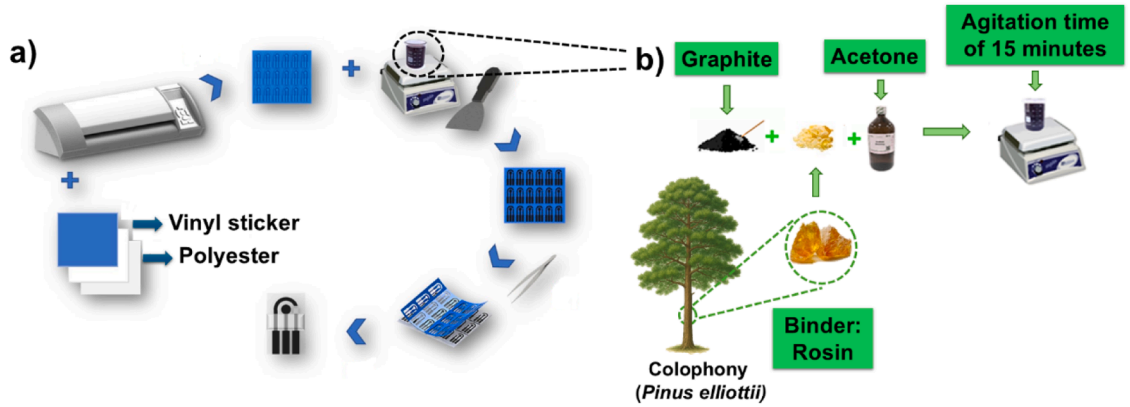

Scheme 1. a) Schematic representation of the GPC-SE printing method. **b)** Preparation of conductive ink using carbon, rosin and acetone for manufacturing the GPC-SE.

2.4. Instrumental and apparatus

Electrochemical measurements were carried out using a μStat 400 bipotentiostat/galvanostat (DropSens, SL, Oviedo, Spain) controlled by DropView 8400 software. The electrochemical behavior of KET at the GPC-SE was investigated by cyclic voltammetry (CV) at different pH values. Prior to each measurement, the GPC-SE was subjected to electrochemical pretreatment by CV at a scan rate of 100 mV s^{-1}, within a potential window from –0.6 to +1.0 V, for 10 scans in 5.0 mol L^{-1} acetic acid solution as described elsewhere [33]. The detection of KET was further optimized and compared using SWV and differential pulse voltammetry (DPV). The SWV voltammograms were processed using OriginPro 2025 software, with baseline corrections applied where appropriate.

Scanning electron microscopy (SEM) and GC–MS analyzes of seized samples were performed as described in the electronic supplementary material (ESM).

2.5. Green analytical chemistry metrics for electrochemical analyses

The environmental sustainability of the proposed electrochemical method, in comparison with conventional approaches, was assessed using the free software AGREE [34].

3. Results and discussion

3.1. Physicochemical characterization of GPC-SE

Different proportions of graphite, rosin, and acetone were investigated for the preparation of the GPC-SE, and the electrochemical response of the sensor was assessed using the $[Fe(CN)_6]^{4-/3-}$ redox couple in 0.1 mol L^{-1} KCl by CV at 50 mV s^{-1}, before and after acid pretreatment of the WE. The choice of 5.0 mol L^{-1} acetic acid, as reported in the literature [33], is consistent with the principles of Green Chemistry, particularly regarding the use of safer reagents and the minimization of waste [35]. As a weak organic acid with low toxicity, high biodegradability, and lower corrosiveness compared to strong mineral acids such as HCl or H_2SO_4, acetic acid is widely recognized as a more environmentally benign alternative [36]. In addition, the use of a reduced volume further contributes to decreasing reagent consumption and waste generation [35]. Despite its mild nature, acetic acid treatment is effective for surface modification of the electrode, promoting the removal of residual impurities and the activation of oxygen-containing functional groups [37]. This enhances surface wettability and electrode–electrolyte interactions without significantly compromising the conductive matrix [37,38]. The electrochemical performance was evaluated in terms of the reversibility of the redox process, considering both the peak-to-peak separation and the anodic-to-cathodic peak current ratio. These parameters, summarized in Tables S1 and S2 and illustrated in Figures S1 and S2, allowed a comparative evaluation of electrode performance. Quality control criteria were applied during the production of the electrode batches to verify the integrity of the electrical connections, the complete formation of the electrodes, and the homogeneity of the coating surface. Electrodes that did not meet these criteria were excluded from subsequent analyses. The best electrochemical response was achieved with a formulation containing 55% graphite and 45% rosin, combined with 5 mL of acetone as solvent. Devices produced under these conditions exhibited low mechanical strength. Structural fragility was observed, particularly at the electrical contacts, which proved to be brittle and prone to failure. Consequently, the formulation containing 5 mL of solvent was selected for subsequent studies, as it enabled the fabrication of devices with improved mechanical integrity, a lower incidence of manufacturing defects, and more reproducible electrochemical performance. In addition, this formulation allowed the production of two blisters, each containing 20 disposable electrodes, thereby increasing the number of units obtained per fabrication batch. Under these conditions, improved signal reversibility and peak current ratios closer to unity were observed, confirming the suitability of this formulation for the fabrication of the GPC-SE. Then, physicochemical characterization of the lab-made electrodes was performed before and after activation, using Raman spectroscopy and SEM (Fig. 1).

Fig. 1a shows the Raman spectra of the GPC-SE electrodes before and after acid treatment, displaying the characteristic bands of graphite-like structures: D (~1332 cm^{-1},), G (~1580 cm^{-1}), and 2D (~2778 cm^{-1}). The calculated I_D/I_G ratios were 0.61 for the untreated GPC-SE and 0.69 for GPC-SE with treatment, indicating a degree of structural disorder in the graphitic materials. The increase in the I_D/I_G ratio for GPC-SE after acid treatment suggests that the acid treatment introduces more structural defects, leading to greater disorder within the graphitic structure [39]. This treatment may also remove part of the binder or modify its conformation, thereby exposing a larger fraction of the active graphite area. SEM images were obtained to analyze the surface morphology of the GPC-SE electrodes without treatment (Fig. 1c) and with treatment (Fig. 1b). As shown in Fig. 1c, the untreated electrode surface consists of a polymeric matrix with small projecting structures, corresponding to the typical carbonaceous morphology, characterized by lighter, spherical features, probably corresponding to binder deposits on the graphite matrix. The smoother regions surrounding these features suggest partial coverage of the graphite surface by the resin. In contrast, the activated electrode (Fig. 1b) exhibited a clear reduction or absence of these spherical aggregates, which may suggest an increase in surface defects.

Electrochemical characterization was initially performed through scan rate studies using representative outer- and inner-sphere redox

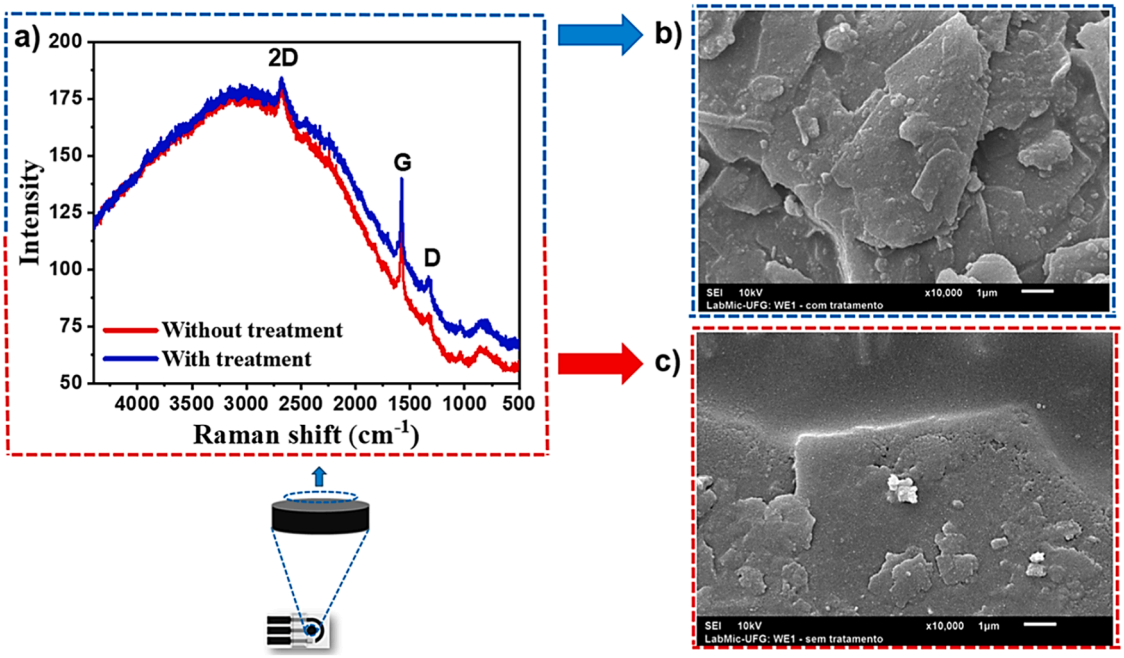

Fig. 1. a) Raman spectra for GPC-SE without treatment in red and with treatment in blue. SEM micrographs for the surface with treatment **b)** and without treatment **c)** at 10 k magnification.

probes, $[Fe(CN)_6]^{4-/3-}$ and $[Ru(NH_3)_6]^{2+/3+}$(1.0 mmol L^{-1} in 0.1 mol L^{-1} KCl), as shown in Fig. 2a-b.

To further investigate mass transport behavior and interfacial sensitivity, two different redox couples were employed, namely the inner-sphere $[Fe(CN)_6]^{4-/3-}$ and the outer-sphere $[Ru(NH_3)_6]^{2+/3+}$ systems. For the ferri/ferrocyanide couple, excellent linearity was obtained for both anodic and cathodic branches, with correlation coefficients of $R^2 = 0.998$ and $R^2 = 0.993$, respectively. The corresponding slopes were 3.59×10^{-5} and -2.84×10^{-5} A $(V\ s^{-1})^{-1/2}$, indicating a diffusion-controlled regime with some dependence on surface-related interactions typical of inner-sphere probes. Similarly, the RuHex couple also displayed a clear diffusion-governed response, with slopes of 4.98×10^{-5} and -4.98×10^{-5} A $(V\ s^{-1})^{-1/2}$ and high linearity ($R^2 = 0.9842$ and $R^2 = 0.9997$), suggesting more efficient electron transfer and reduced sensitivity to surface functional groups, consistent with its outer-sphere character [40,41].

The electroactive surface area was estimated using the Randles–Ševčík equation for quasi-reversible systems [42,43]. The heterogeneous electron transfer rate constant (k_o) was determined using the Nicholson method [42,43], based on potential scan rate studies conducted from 5 to 500 mV s^{-1}. Fig. 2 also presents the corresponding Randles–Ševčík plots. For GPC-SE, k_o was calculated as 1.24 ± 0.04 ($\times 10^{-3}$) cm s^{-1}, and the electroactive surface area was determined to be 0.06 ± 0.004 cm^2.

Additionally, the SPC-SE electrodes were characterized by electrochemical impedance spectroscopy (EIS) performed in the presence of $[Fe(CN)_6]^{4-/3-}$ over a frequency range of 0.05 – 200 000 Hz. EIS provides complementary information on the resistive and interfacial properties of the electrode by allowing the evaluation of the solution resistance (R_s) and the charge transfer resistance (R_{ct}). The experimental data were fitting using a Randles-type equivalent circuit (solution resistance, interfacial charge-transfer resistance, non-ideal double-layer capacitance and Warburg), which is appropriate or carbon-based electrodes probed with fast outer-sphere redox couples, where the impedance response is governed primarily by electrolyte resistance, charge-transfer kinetics, and non-ideal double-layer capacitance. The Nyquist and Bode plots for the SPC-SE after treatment are shown in Fig. 2c and 2d, respectively.

The Nyquist representation was used to extract quantitative values of R_S and R_{CT}, yielding of $1510 \pm 70\Omega$ and an $43.7 \pm 3k\Omega$, respectively, indicating improved interfacial charge-transfer properties after acid treatment. The Bode plots were included as complementary data to confirm the presence of a single dominant time constant and support the validity of the equivalent circuit selection. Impedance spectra recorded for electrodes without acid treatment did not exhibit a well-defined semicircle or phase behavior suitable for reliable fitting, preventing meaningful extraction of electrochemical parameters. This result further supports the role of the pre-treatment step in enabling reproducible and electrochemically active interfaces. Overall, the EIS analysis corroborates the enhancement of interfacial properties induced by the activation process, in agreement with the voltammetric characterization.

3.2. *Electroanalytical determination of KET*

3.2.1. *Electrochemical behavior of KET*

Preliminary experiments were conducted to investigate the electrochemical behavior of KET using CV. As shown in Figure S3, KET displayed two irreversible oxidation processes on GPC-SE over the pH range 6 to 12. The oxidation processes exhibited pH-dependent behavior, as the peak potential (E_p) decreased with increasing pH values (Figure S4a) up to pH 8.0. This difference is likely related to its pKa of KET (7.29), as the molecule exists predominantly in its deprotonated form at pH $\geq$ 6 [44]. The pH value of 8.0 was selected for KET detection on GPC-SE as it yielded the best resolution between P1 and P2 peaks (Figure S4b). BR, phosphate, and borate buffers were subsequently evaluated (Figure S5). Interestingly, BR yielded the most well-defined peaks and was therefore selected as the supporting electrolyte for KET detection throughout this study. Different BR concentrations were then tested to assess the effect of ionic strength on KET detection, with 0.05 mol L^{-1} BR providing the optimal resolution of the observed oxidation processes (Figure S6).

Subsequently, scan rate experiments were conducted to evaluate the mass transport control of the P1 at 0.62 V and P2 at 0.90 V (vs. Ag) processes at GPC-SE surface (Figure S7). The peak currents (I_p) for P1 and P2 exhibited a stronger linear correlation with the square root of the frequency ($R^2 = 0.80$ and 0.81) than with the frequency alone ($R^2 = 0.77$

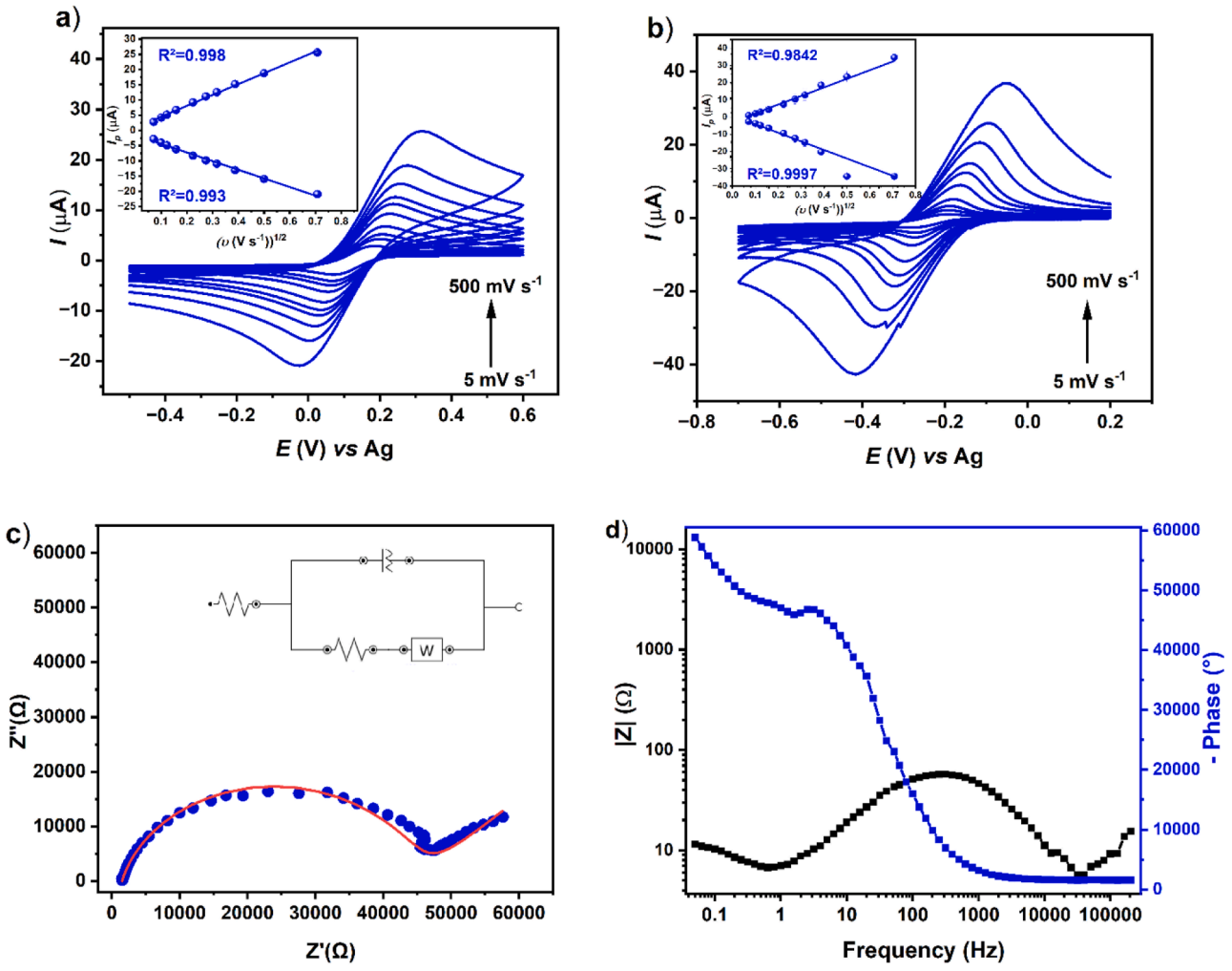

Fig. 2. Scan rate study (5 – 500 mV s^{-1}) with $[Fe(CN)_6]^{4-/3-}$ ***a)*** and $[Ru(NH_3)_6]^{2+/3+}$ ***b)*** (both 1 mmol L^{-1} in 0.1 mol L^{-1} KCl) performed on GPC-SE. Inset: the Randles–Ševčík plot. EIS Nyquist **c)** and Bode **d)** plots of $[Fe(CN)_6]^{4-/3-}$. Inset: the proposed equivalent circuit.

and 0.74), indicating that the redox processes are predominantly diffusion-controlled, which is further supported by the logarithmic plot (Figure S7).

Recent liquid chromatography–quadrupole time-of-flight mass spectrometry (LC–QTOF-MS) studies confirmed that the initial oxidation of KET leads to the formation of norketamine via demethylation, dehydroketamine via double-bond formation, and hydroxylated KET derivatives, analogous to the metabolic products of KET [45]. The number of electrons involved was estimated to be $-2e^-$ using $-2H^+$. At more positive potentials corresponding to the second oxidation peak (P2), additional products were observed, including an N-formyl derivative and a chlorinated derivative, likely resulting from further oxidation of the initial products near the electrode surface [45]. The formation of these products explains the lower intensity and lack of reproducibility of the second oxidation peak observed in the voltammetric scans; consequently, only the first oxidation peak (P1) was used for the detection and quantification of KET using the proposed method [45]. These findings confirm the occurrence of two distinct irreversible oxidation processes, consistent with the voltammetric behavior observed in this study, and provide additional insights into the oxidation mechanism of KET.

3.2.2. *KET detection by SWV on GPC-SE*

The DPV and SWV techniques were optimized and compared under the following optimal conditions: amplitude, 0.05 V; step, 0.01 V; time interval, 0.3 s; and modulation time, 10 ms for DPV; and amplitude, 0.05 V; step, 0.01 V; and frequency, 20 Hz for SWV. The optimal parameters were selected based on the relationship between peak height and peak width at half-height. Figure S8 presents the comparison between the two techniques, KET. SWV produced better-defined peaks and was therefore selected for subsequent experiments, in this condition KET exhibits two irreversible oxidations at potentials +0.59 V and 0.77 V vs. Ag. Under optimized experimental conditions, the repeatability of the method was evaluated through intra-electrode studies performed in triplicate, consisting of three consecutive measurements using the same electrode. Reproducibility was also assessed in triplicate using three distinct electrodes obtained from the same fabrication batch, allowing the evaluation of both inter-electrodes. The proposed method exhibited consistent responses across different assays performed within the same time interval, with low relative standard deviations (RSD) for peak potential (E_P < 2.0%) and peak current (I_P< 5.0%), shown in Figure S9a. These results demonstrate good repeatability and reproducibility within the stability window of the batch, confirming the reliability of the electrochemical response associated with the KET oxidation process. The long-term stability of the electrode was evaluated up to 15 days after the manufacture of the SPC-SEs, as shown in Figure S9b. The GPC-SE exhibited stable peak potential and peak currents for the P1 and P2 oxidation processes of KET for up to 10 days after fabrication, with RSDs of 0.99% and 2.86% for E_p, and 5.86% and 8.48% for I_p, respectively. After 15 days, a significant decrease in the P1 peak current (40%) was

observed, indicating that beyond this period the electrode remains suitable for qualitative identification of KET but presents limitations for accurate quantitative analysis.

The determination of KET using GPC-SE was evaluated over a concentration range of 50 – 500 μmol L^{-1} in BR buffer solution (pH 8.0, 0.05 mol L^{-1}). The corresponding voltammograms are shown in Fig. 3.

As shown in Fig. 3, a linear range ($R^2 = 0.999$) between 50 and 500 μmol L^{-1} was obtained for KET quantification using P1, with linear regression: I_{pa} (μA) = −0.1203 + 0.0045 × *[KET]* μmol L^{-1}. The limits of detection (LOD) and quantification (LOQ) were calculated according to $3S_b/m$ and $10S_b/m$, respectively [46], where S_B denotes the standard deviation (n= 10) of the background (blank) signal, and m is the slope of the calibration curve, yielding values of 3.3 and 10.1 μmol L^{-1}. It is important to highlight that a wide range of concentrations was evaluated, although KET was detected in seized samples containing approximately 20 to 300 mg per unit, according to data from the DrugsData database (Erowid Center) [47]. Showing that the proposed method can be applied to seized samples and biological samples from poisoning cases containing KET. The highest incidence was observed in the 100 to 300 mg range [47], evidencing the lack of standardization in formulations and possible variations in the purity and degree of dilution of the analyzed samples. These results reinforce the need for complementary laboratory analyses to determine the actual content of the active substance and to assess potential toxicological risks, in addition to demonstrating the feasibility and suitability of the proposed method for the identification and quantification of KET using SWV combined with GPC-SE.

3.2.3. *Interference study and determination in forensic samples*

To assess the practical applicability of the proposed method in beverage, biological, and real seized samples, an interference study was performed to evaluate the detection of other drugs, including MDMA, procaine, lidocaine, cocaine, mephedrone, morphine, and methadone, as well as a common adulterant, paracetamol. The results of these interference studies are shown in Fig. 4, with a comparison of the KET electrochemical signal highlighted in all graphs (red line).

In the comparative analysis with other drugs and pharmaceuticals (Fig. 4), it was observed that compounds such as paracetamol (+0.28 V) and morphine (+0.18 V) present oxidation potentials sufficiently separated from the KET peak (+0.59 V and 0.77 V vs. Ag.), allowing their

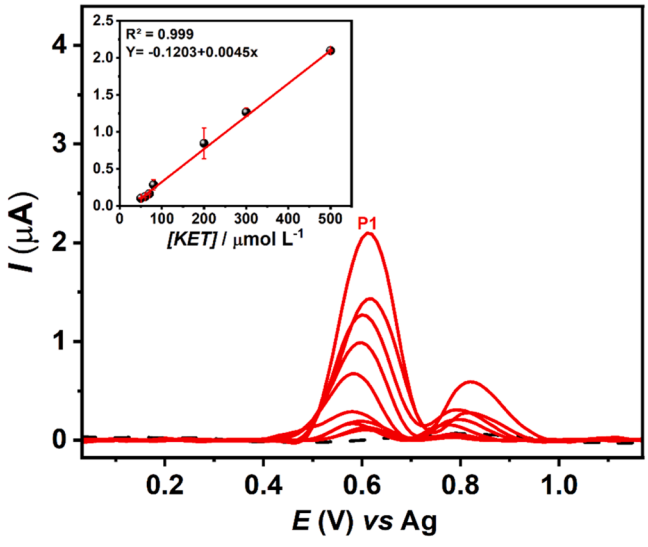

Fig. 3. Square-wave voltammograms in 0.05 mol L^{-1} BR buffer solution at pH 8.0 (blank: black line) on GPC-SE before and after addition of 50 – 500 μmol L^{-1} KET. The inset shows linear regression. All measurements were performed in triplicate. Experimental conditions: amplitude of 0.05 V, step potential 0.01 V, and frequency 20 Hz.

discrimination in complex samples. Substances such as lidocaine (+0.69 V) and procaine (+0.71 V) present a different electrochemical profile, with only one oxidation, therefore the P2 of KET can be used for selective determination. However, MDMA (+0.60 / +0.94 V), cocaine, mephedrone, and methadone exhibit overlapping or very close oxidation potentials, which may lead to analytical interferences at higher concentrations. Accordingly, selectivity was evaluated through differences in oxidation peak potentials and voltammetric profiles, and peak discrimination was assessed qualitatively using superimposed voltammograms.

It is important to note that MDMA and cocaine may interfere with the electrochemical analysis of KET, particularly at high concentrations, as these substances have previously been reported in seized samples containing KET [48]. However, this does not represent a limitation for drug control applications, since these compounds are themselves of forensic relevance and require monitoring. The proposed electrochemical method exhibits enhanced selectivity by enabling discrimination based on oxidation potential, allowing KET to be distinguished from several commonly encountered drugs. Even when partial peak overlaps occur, the ability to resolve electroactive species provides an advantage over conventional colorimetric screening methods. The selectivity arises from the combined effect of the electrode material, surface treatment, and electrochemical detection strategy. The feasibility of the proposed method across different matrices was demonstrated through analyses of artificial saliva, synthetic urine, human serum, and vitreous humor, as well as alcoholic beverages (whisky and wine) and real seized samples (Figs. 5 and S10).

Figs. 5 and S10 demonstrate that the electrochemical behavior of KET in biological matrices, beverages, and seized samples was consistent with that observed for the standard compound. Although the wine sample exhibited only a single well-defined voltammetric peak for KET (P1), this difference can be attributed either to a matrix effect associated with the complex chemical composition of wine [49,50] or to the fact that peak P2 corresponds to an intrinsically poorly reproducible electrochemical process [45].

Seized sample 1 (Fig. 5b), containing KET, caffeine, and eutylone, previously confirmed by GC–MS (Figure S11), was successfully identified and quantified using the proposed method with the GPC-SE, resulting in a KET concentration of 5.78 mg. Although this value is lower than those reported by the UNODC for seized tablets [6], this discrepancy can be attributed to the presence of other adulterants, such as caffeine and eutylone. Thus, the proposed method demonstrated significant efficiency for the identification of KET in complex matrices, including seized tablets, saliva, urine, vitreous humor, and serum. As shown in Table S3 and Figure S10b, KET could be quantified in all matrices using peak P1, with the exception of wine and whisky, which showed recoveries above 120%. Small background variations in complex matrices can be a potential source of variability. Nevertheless, the biological samples exhibited recoveries of approximately 97 (±5)%, indicating that the proposed method can be reliably applied to forensic analyses under real conditions.

The evaluation of the electrochemical method using the AGREE software resulted in an overall score of 0.87 (Figure S10c), demonstrating strong compliance with the Green Analytical Chemistry principles. The method exhibited notable advantages, including low sample consumption, minimal waste generation, reduced toxicity, high operator safety, lower energy demand, and potential for miniaturization. The main limitation identified was the requirement for specific reagents; however, overall, the method represents a sustainable and efficient analytical alternative. Table 1 presents a comparison of the main analytical parameters for KET determination using electroanalytical methods and carbon-based electrodes reported to date.

When comparing the analytical parameters of the developed method (GPC-SE – SWV) with those reported in the literature (Table 1), it can be observed that the linear range obtained (50 – 500 μmol L^{-1}) is comparable to that achieved by other methods based on SPEs [25]. Although

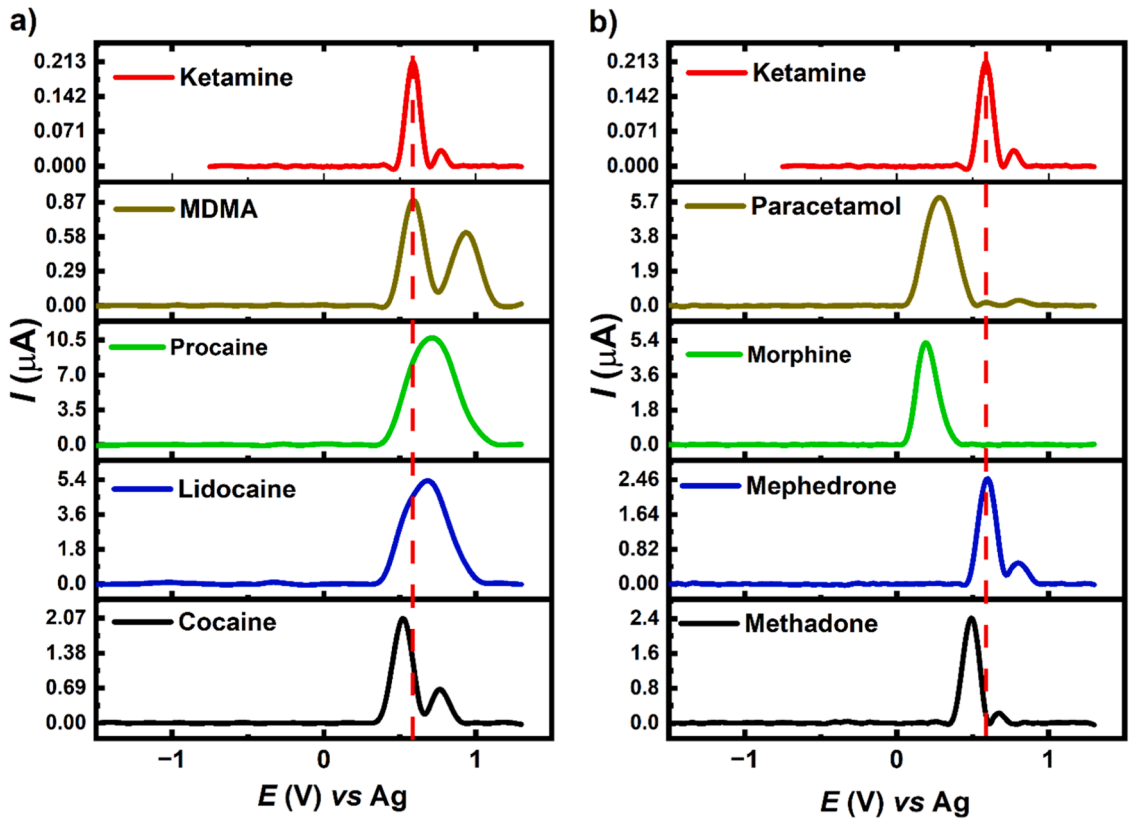

Fig. 4. a) SWVs voltammograms for MDMA, procaine, lidocaine and cocaine **b)** and for paracetamol, morphine, mephedrone, methadone. Compared with KET on GPC-SE. All compounds were at a concentration of 80 μmol L^{-1} in 0.05 mol L^{-1} BR buffer solution pH 8.0. The experimental conditions were the same as in Fig. 3.

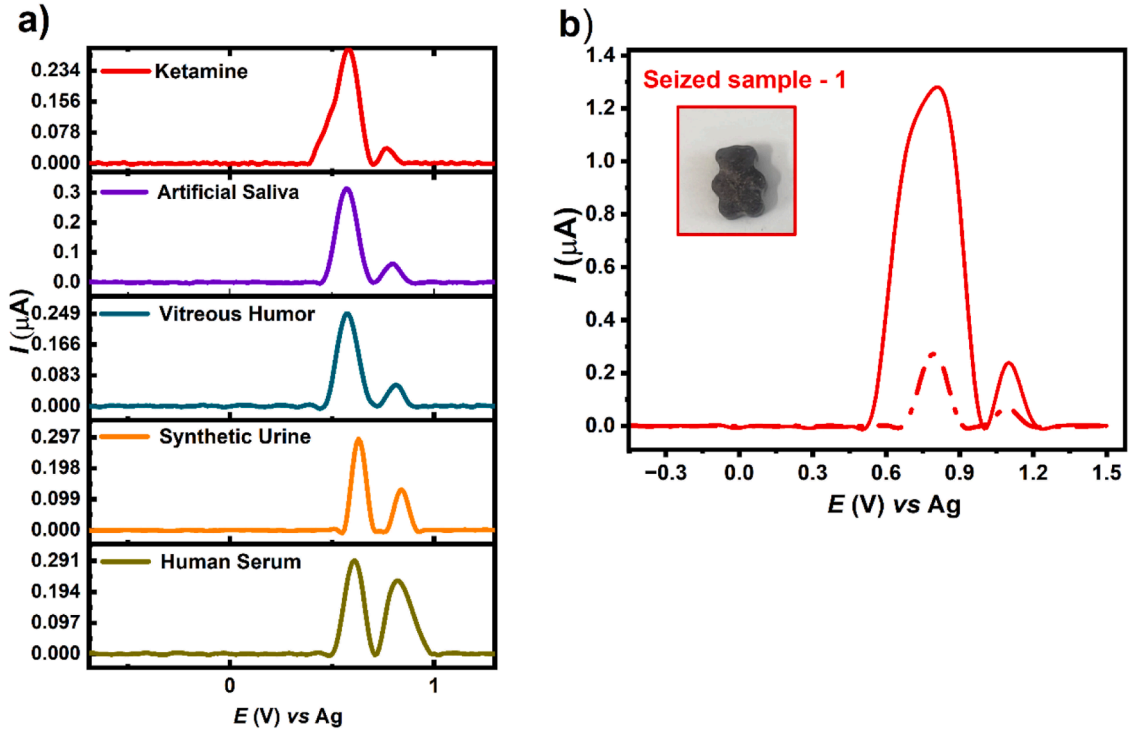

Fig. 5. a) SWV voltammograms on GPC-SE obtained for artificial saliva, vitreous humor, synthetic urine, and human serum **b)** and seized samples containing KET, caffeine, and eutylone. The experimental conditions were the same as in Fig. 3. before and after addition of 80 μmol L^{-1} KET in BR buffer solution 0.05 mol L^{-1} (pH 8.0).

the limit of detection (LOD) (3.3 μmol L^{-1}) is higher than those reported for PGE-SWV and SPE-MOFs@G-DPV, it remains suitable for practical

Table 1
Comparison of analytical parameters for KET detection by electrochemical methods.

Electrode	Method	Linear Range (μmol L^{-1})	LOD (μmol L^{-1})	Reference
PGE	SWV	0.001 – 1.0	0.0007	[51]
EMC	EIS	7.3 – 3600	1.8	[52]
SPE	DPV	50 – 500	15	[25]
SPE - ItalSens IS-C	SWV	50 – 2500	11.7	[45]
SPE - (MOFs@G)	DPV	0.0001 – 40	4.0×10^{-5}	[26]
GPC-SE	SWV	50 – 500	3.3	This work

PGE: Pencil-type graphite electrode; EMC: Chemically modified electrode; SPE: Commercially available graphite screen-printed electrodes; SPE: ItalSens IS-C disposable graphite electrodes; SPE: Screen-printed electrode modified with a metal-organic framework/graphene nanocomposite (MOFs@G); GPC-SE: Graphite-pine rosin composite stencil electrode.

applications, particularly in seized samples where KET concentrations are typically higher.

Moreover, the GPC-SE electrode offers significant advantages in terms of sustainability and cost-effectiveness. Fabricated from low-cost materials and potentially reusable, it meets current demands for greener analytical methods by reducing waste generation and minimizing the need for sophisticated reagents or complex modification steps required for electrodes based on MOFs or graphene. Therefore, although the LOD is not the lowest among the compared methods, the combination of an appropriate linear range, operational simplicity, low cost, and sustainable design makes the proposed electrode a promising and environmentally responsible alternative for routine KET analysis in real forensic samples.

4. Conclusion

This study presents a novel electrochemical approach that establishes a robust analytical platform for forensic investigations involving KET, whether related to intoxication or illicit use. The lab-made GPC-SE electrode, composed of graphite, rosin, and acetone, employs rosin as a sustainable and efficient binder, delivering improved performance compared to conventional formulations. Using square-wave voltammetry, KET was rapidly detected in beverages, biological matrices, and seized samples, achieving a LOD of 3.3 μmol L^{-1} with satisfactory reproducibility (RSD $< 3.0\%$ for E_p and $< 10.0\%$ for I_p). The method requires only 60 μL of sample, enabling portable, on-site analyses while ensuring reliable results. By integrating rosin as a green binder, the proposed electrode provides a sustainable, low-cost, and high-performance alternative for electrochemical sensing. Overall, this study introduces an innovative electrode design and validates its applicability in forensic contexts, providing a rapid and environmentally friendly tool for the detection and quantification of KET in complex matrices.

CRediT authorship contribution statement

Jamilson P. Campos: Writing – original draft, Visualization, Validation, Methodology, Investigation, Formal analysis, Data curation, Conceptualization. **Larissa M.A. Melo:** Writing – review & editing, Writing – original draft, Visualization, Methodology, Investigation, Formal analysis, Data curation, Conceptualization. **Danielly S. Rocha:** Methodology, Investigation. **Daniel Júnior A. dos Santos:** Writing – review & editing, Methodology, Investigation. **Maurício M.L. Pereira:** Methodology, Investigation. **Wallans T.P. dos Santos:** Writing – review & editing, Visualization, Resources, Conceptualization. **Luciano C. Arantes:** Writing – review & editing, Visualization, Resources, Investigation, Conceptualization. **Wendell K.T. Coltro:** Writing – review & editing, Supervision, Resources, Project administration, Funding acquisition, Conceptualization.

Declaration of competing interest

The authors declare that they have no known competing financial interests or personal relationships that could have appeared to influence the work reported in this paper.

Acknowledgements

The authors would like to thank CNPq (grant 308136/2025-0, 308152/2025-5, and 406309/2025-6), FAPEMIG (grants PPM-00142-18, APQ-01996-23 and RED-00120-23), FAPEG (grants 202310267000258 and 202310267000560), INCT-SP (grant 406958/2022-0) and INCTBio (grant 408338/2024-5) for their financial support. The PCDF is also recognized for the collaboration, donation of seized samples, and support in the development of this study. Lastly, the authors acknowledge the Multiuser Laboratory of High-Resolution Microscopy (LabMic/UFG) for using their facilities and Dr. Thiago M.G. Cardoso for the helpful discussion in the initial stage of this project.

Supplementary materials

Supplementary material associated with this article can be found, in the online version, at doi:10.1016/j.electacta.2026.148448.

Data availability

Data will be made available on request.

References

[1] J.-H. Li, B. Vicknasingam, Y. Cheung, W. Zhou, A.W. Nurhidayat, D.C. Des Jarlais, R. Schottenfeld, To use or not to use: an update on licit and illicit ketamine use, Subst. Abuse Rehabil. 2 (2011) 11–20, https://doi.org/10.2147/SAR.S15458.
[2] E. Han, N. ji Kwon, L.Y. Feng, J.H. Li, H. Chung, Illegal use patterns, side effects, and analytical methods of ketamine, Forensic Sci. Int. 268 (2016) 25–34, https://doi.org/10.1016/J.FORSCIINT.2016.09.001.
[3] J.M. Pappachan, B. Raj, S. Thomas, F.W. Hanna, Multiorgan dysfunction related to chronic ketamine abuse, Proc. (Bayl Univ. Med. Cent.) 27 (2014) 223, https://doi.org/10.1080/08998280.2014.11929117.
[4] M.R. Varì, G. Ricci, M. Cavallo, S. Pichini, A. Sirignano, S. Graziano, Ketamine: from prescription anaesthetic to a new psychoactive substance, Curr. Pharm. Des. 28 (2022) 1213–1220, https://doi.org/10.2174/1381612828666220510115209.
[5] S. Pichini, F.P. Busardò, A. Gregori, P. Berretta, S. Gentili, R. Pacifici, Purity and adulterant analysis of some recent drug seizures in Italy, Drug Test. Anal. 9 (2017) 485–490, https://doi.org/10.1002/DTA.2134.
[6] UNODC - United Nations Office on drugs and crime, synthetic drugs in East and Southeast Asia. https://www.unodc.org/roseap/uploads/documents/Publications/2024/Synthetic_Drugs_in_East_and_Southeast_Asia_2024.pdf, 2024 accessed September 18, 2025.
[7] A. Florea, M. de Jong, K. De Wael, Electrochemical strategies for the detection of forensic drugs, Curr. Opin. Electrochem. 11 (2018) 34–40, https://doi.org/10.1016/J.COELEC.2018.06.014.
[8] S. Monteiro, J.C. Santos Júnior, E.M. Sussuchi, Virtual Quim. |vol 12| |No. 5| | 1145-1160| rev, Virtual Quim. (n.d) (2020) 1145–1160, https://doi.org/10.21577/1984-6835.20200092.
[9] L.M.A. Melo, L.V. de Faria, L.C. Arantes, M. Vojs, M. Marton, R.F. Brocenschi, E. M. Richter, R.A.A. Munoz, W.T.P. dos Santos, Use of a lab-made screen-printed sensor with chemically deposited boron-doped diamond for simple and selective electrochemical detection of the synthetic cathinone N-ethylpentylone in forensic samples, Electrochim. Acta 465 (2023) 142996, https://doi.org/10.1016/J.ELECTACTA.2023.142996.
[10] K.R. Teófilo, L.C. Arantes, P.A. Marinho, A.A. Macedo, D.M. Pimentel, D.P. Rocha, A.C. de Oliveira, E.M. Richter, R.A.A. Munoz, W.T.P. dos Santos, Electrochemical detection of 3,4-methylenedioxymethamphetamine (ecstasy) using a boron-doped diamond electrode with differential pulse voltammetry: simple and fast screening method for application in forensic analysis, Microchem. J. 157 (2020) 105088, https://doi.org/10.1016/J.MICROC.2020.105088.
[11] D.S. Araújo, L.C. Arantes, L.V. Faria, K.A.O. Souza, D.M. Pimentel, S.L. Barbosa, E. M. Richter, R.A.A. Muñoz, W.T.P. dos Santos, Electrochemistry of 5F-MDMB-PICA synthetic cannabinoid using a boron-doped diamond electrode with short anodic-cathodic pretreatment: a simple screening method for application in forensic analysis, Electrochim. Acta 454 (2023) 142356, https://doi.org/10.1016/J.ELECTACTA.2023.142356.
[12] L.M.A. Melo, L.C. Arantes, D.M. Pimentel, A.A. Macedo, R.M. Verly, E.S. Gil, W.T. P. dos Santos, Electrochemistry of the synthetic tryptamine 5-MeO-MiPT at glassy carbon and screen-printed electrodes: a rapid and simple screening method for

application in forensic analysis, Sens. Actuators B Chem. 393 (2023) 134183, https://doi.org/10.1016/J.SNB.2023.134183.
[13] L.M.A. Melo, L.V. de Faria, L.C. Arantes, E.M. Richter, R.A.A. Munoz, W.T.P. dos Santos, Combined colorimetric and electrochemical screening method using 3D printed devices: towards the selective detection of MDMA in forensic samples, Electrochim. Acta 483 (2024) 144041, https://doi.org/10.1016/J.ELECTACTA.2024.144041.
[14] L.V. de Faria, R.G. Rocha, L.C. Arantes, D.L.O. Ramos, C.D. Lima, E.M. Richter, W. T.P dos Santos, R.A.A. Muñoz, Cyclic square-wave voltammetric discrimination of the amphetamine-type stimulants MDA and MDMA in real-world forensic samples by 3D-printed carbon electrodes, Electrochim. Acta 429 (2022) 141002, https://doi.org/10.1016/J.ELECTACTA.2022.141002.
[15] L.V. de Faria, A.A. Macedo, L.C. Arantes, T.A. Matias, D.L.O. Ramos, E.M. Richter, W.T.P. dos Santos, R.A.A. Muñoz, Novel disposable and portable 3D-printed electrochemical apparatus for fast and selective screening of 25E-NBOH in forensic samples, Talanta 269 (2024) 125476, https://doi.org/10.1016/J.TALANTA.2023.125476.
[16] R.G. Rocha, J.S. Ribeiro, M.H.P. Santana, E.M. Richter, R.A.A. Muñoz, 3D-printing for forensic chemistry: voltammetric determination of cocaine on additively manufactured graphene–polylactic acid electrodes, Anal. Methods 13 (2021) 1788–1794, https://doi.org/10.1039/D1AY00181G.
[17] A.F. João, R.G. Rocha, T.A. Matias, E.M. Richter, J. Flávio, S. Petruci, R.A. A. Muñoz, 3D-printing in forensic electrochemistry: atropine determination in beverages using an additively manufactured graphene-polylactic acid electrode, Microchem. J. 167 (2021) 106324, https://doi.org/10.1016/J.MICROC.2021.106324.
[18] P. Kelíšková, O. Matvieiev, L. Janíková, R. Šelešovská, Recent advances in the use of screen-printed electrodes in drug analysis: a review, Curr. Opin. Electrochem. 42 (2023) 101408, https://doi.org/10.1016/J.COELEC.2023.101408.
[19] M.A. Balbino, É.N. Oiye, M.F.M. Ribeiro, J.W.C. Júnior, I.C. Eleotério, A.J. Ipólito, M.F. de Oliveira, Use of screen-printed electrodes for quantification of cocaine and Δ9-THC: adaptions to portable systems for forensic purposes, J. Solid State Electrochem. 20 (2016) 2435–2443, https://doi.org/10.1007/S10008-016-3145-3/METRICS.
[20] G. Murilo Alves, A. Soares Castro, B.R. McCord, M.F. de Oliveira, MDMA electrochemical determination and behavior at carbon screen-printed electrodes: cheap tools for forensic applications, Electroanalysis 33 (2021) 635–642, https://doi.org/10.1002/ELAN.202060080;WGROUP:STRING:PUBLICATION.
[21] A.A. Macedo, L.C. Arantes, D.M. Pimentel, T. de Deus Melo, L. Magalhães de Almeida Melo, W. Alves de Barros, C.M. Rocha, Â.de Fátima, W.T. Pio dos Santos, Comprehensive detection of lysergic acid diethylamide (LSD) in forensic samples using carbon nanotube screen-printed electrodes, Anal. Methods 15 (2023) 5837–5845, https://doi.org/10.1039/D3AY01385E.
[22] A.A. Macedo, D.M. Pimentel, L.M. de A. Melo, C.M. Rocha, Â.de Fátima, K.A. O. Souza, J.L. Costa, L.C. Arantes, W.T.P. dos Santos, Environmentally friendly screen-printed electrodes for the selective detection of 4-bromo-2,5-dimethoxy-phenethylamine (2C-B) in forensic analysis, Anal. Methods 16 (2024) 7633–7642, https://doi.org/10.1039/D4AY01310G.
[23] M.O.B. Arrieiro, L.C. Arantes, D.A.R. Moreira, D.M. Pimentel, C.D. Lima, L.M. F. Costa, R.M. Verly, W.T.P. dos Santos, Electrochemical detection of eutylone using screen-printed electrodes: rapid and simple screening method for application in forensic samples, Electrochim. Acta 412 (2022) 140106, https://doi.org/10.1016/J.ELECTACTA.2022.140106.
[24] C.D. Lima, L. Magalhães de Almeida Melo, L.C. Arantes, N. dos S. Conceição, I. de França Schaffel, L.L. Machado, R. de Queiroz Ferreira, W.T. Pio dos Santos, Simple and selective screening method for the synthetic cathinone MDPT in forensic samples using carbon nanofiber screen-printed electrodes, Talanta 269 (2024) 125375, https://doi.org/10.1016/J.TALANTA.2023.125375.
[25] P. Stelmaszczyk, K. Białkowska, K. Sekuła, R. Stanaszek, R. Wietecha-Posłuszny, Screen-printed electrode-based sensor for rapid ketamine determination: optimization and on-site application for seized drugs analysis, Monatsh. Chem. 155 (2024) 881–888, https://doi.org/10.1007/S00706-024-03237-W/TABLES/2.
[26] K. Fu, R. Zhang, J. He, H. Bai, G. Zhang, Sensitive detection of ketamine with an electrochemical sensor based on UV-induced polymerized molecularly imprinted membranes at graphene and MOFs modified electrode, Biosens. Bioelectron. 143 (2019) 111636, https://doi.org/10.1016/J.BIOS.2019.111636.
[27] S.J. Kim, B.R. Lee, E.S. Oh, Application of a bio-derivative, rosin, as a binder additive for lithium titanium oxide electrodes in lithium-ion batteries, J. Power Sources 273 (2015) 608–612, https://doi.org/10.1016/J.JPOWSOUR.2014.09.160.
[28] C. Qian, X. Wu, F. Zhang, W. Yu, Electrochemical impedance investigation of Ni-free Co-Cr-Mo and Co-Cr-Mo-Ni dental casting alloy for partial removable dental prosthesis frameworks, J. Prosthet. Dent. 116 (2016) 112–118, https://doi.org/10.1016/j.prosdent.2015.12.001.
[29] N. Laube, B. Mohr, A. Hesse, Laser-probe-based investigation of the evolution of particle size distributions of calcium oxalate particles formed in artificial urines, J. Cryst. Growth 233 (2001) 367–374, https://doi.org/10.1016/S0022-0248(01)01547-0.
[30] S.S. Thakur, S.K. Shenoy, J.S. Suk, J.S. Hanes, I.D. Rupenthal, Validation of hyaluronic acid-agar-based hydrogels as vitreous humor mimetics for in vitro drug and particle migration evaluations, Eur. J. Pharm. Biopharm. 148 (2020) 118–125, https://doi.org/10.1016/J.EJPB.2020.01.008.
[31] C. Cole, L. Jones, J. McVeigh, A. Kicman, Q. Syed, M. Bellis, Adulterants in illicit drugs: a review of empirical evidence, Drug Test. Anal. 3 (2011) 89–96, https://doi.org/10.1002/DTA.220.
[32] D. Santos Rocha, A. Silva-Neto, C. De Oliveira, S. Gonçalves, G. Souza, M. Henrique, P. Santana, W. Karlos, T. Coltro, Disposable stencil-printed carbon electrodes for electrochemical analysis of Sildenafil citrate in commercial and adulterated tablets, Braz. J. Anal. Chem. (n.d) (2022) 210–228, https://doi.org/10.30744/brjac.2179-3425.AR-65-2021.
[33] H.A. Silva-Neto, G.F. Duarte-Junior, D.S. Rocha, F. Bedioui, A. Varenne, W.K. T. Coltro, Recycling 3D printed residues for the development of disposable paper-based electrochemical sensors, ACS Appl. Mater. Interfaces (2023), https://doi.org/10.1021/ACSAMI.3C00370.
[34] F. Pena-Pereira, W. Wojnowski, M. Tobiszewski, AGREE - analytical GREEnness metric approach and software, Anal. Chem. 92 (2020) 10076–10082, https://doi.org/10.1021/ACS.ANALCHEM.0C01887/ASSET/IMAGES/LARGE/AC0C01887_0003.JPEG.
[35] B. Martinengo, E. Diamanti, E. Uliassi, M.L. Bolognesi, Harnessing the 12 green chemistry principles for sustainable antiparasitic drugs: toward the one health approach, ACS Infect. Dis. 10 (2024) 1856, https://doi.org/10.1021/ACSINFECDIS.4C00172.
[36] D. Prat, A. Wells, J. Hayler, H. Sneddon, C.R. McElroy, S. Abou-Shehada, P.J. Dunn, CHEM21 selection guide of classical- and less classical-solvents, Green Chem. 18 (2015) 288–296, https://doi.org/10.1039/C5GC01008J.
[37] A. Ferrari, J. Robertson, Interpretação de espectros Raman de carbono desordenado e amorfo, Phys. Rev. B 61 (2000) 14095, https://doi.org/10.1103/PhysRevB.61.14095.
[38] R. Jiménez-Pérez, M.I. González-Sánchez, A. Gomis-Berenguer, J. Iniesta, E. Valero, Enhanced surface properties and electrochemical performance of carbon-based screen-printed electrodes via hydrogen peroxide activation, Electrochim. Acta 536 (2025) 146721, https://doi.org/10.1016/J.ELECTACTA.2025.146721.
[39] A.C. Ferrari, Raman spectroscopy of graphene and graphite: disorder, electron–phonon coupling, doping and nonadiabatic effects, Solid State Commun. 143 (2007) 47–57, https://doi.org/10.1016/J.SSC.2007.03.052.
[40] J. Huang, Diffusion impedance of electroactive materials, electrolytic solutions and porous electrodes: warburg impedance and beyond, Electrochim. Acta 281 (2018) 170–188, https://doi.org/10.1016/J.ELECTACTA.2018.05.136.
[41] R. Agarwal, The Nicholson method of determination of the standard rate constant of a quasireversible redox couple employing cyclic voltammetry: everything one needs to know!, ACS Electrochem. 1 (2025) 1885–1894, https://doi.org/10.1021/ACSELECTROCHEM.5C00214.
[42] S.J. Rowley-Neale, D.A.C. Brownson, C.E. Banks, Defining the origins of electron transfer at screen-printed graphene-like and graphite electrodes: MoO2 nanowire fabrication on edge plane sites reveals electrochemical insights, Nanoscale 8 (2016) 15241–15251, https://doi.org/10.1039/C6NR04220A.
[43] R.S. Nicholson, Theory and application of cyclic voltammetry for measurement of electrode reaction kinetics, Anal. Chem. 37 (1965) 1351–1355, https://doi.org/10.1021/AC60230A016/ASSET/AC60230A016.FP.PNG_V03.
[44] Chemicalize - soluções instantâneas de Quimioinformática, (n.d.). https://chemicalize.com/app/calculation (accessed September 2, 2025).
[45] J. Schram, M. Parrilla, N. Sleegers, N. Samyn, S.M. Bijvoets, M.W.J. Heerschop, A. L.N. Van Nuijs, K. De Wael, Identifying electrochemical fingerprints of ketamine with voltammetry and liquid chromatography-mass spectrometry for its detection in seized samples, Anal. Chem. 92 (2020) 13485–13492, https://doi.org/10.1021/acs.analchem.0c02810.
[46] The IUPAC Compendium of Chemical Terminology, The IUPAC Compendium of Chemical Terminology (2025). https://doi.org/10.1351/GOLDBOOK.
[47] DrugsData.Org: resultados dos testes, (n.d.). https://www.drugsdata.org/results.php?search_field=substance&s=ketamine (accessed October 24, 2025).
[48] DrugsData.Org: resultados dos testes, (n.d.). https://www.drugsdata.org/results.php?search_field=all&s=ketamine+ (accessed September 18, 2025).
[49] D. Hernanz-Vila, M.J. Jara-Palacios, M.L. Escudero- Gilete, F.J. Heredia, D. Hernanz-Vila, M.J. Jara-Palacios, M.L. Escudero- Gilete, F.J. Heredia, Applications of voltammetric analysis to wine products, applications of the voltammetry (2017). https://doi.org/10.5772/67696.
[50] P.A. Kilmartin, H. Zou, A.L. Waterhouse, A cyclic voltammetry method suitable for characterizing antioxidant properties of wine and wine phenolics, J. Agric. Food Chem. 49 (2001) 1957–1965, https://doi.org/10.1021/JF001044U.
[51] B. Deiminiat, G.H. Rounaghi, Fabrication of a new electrochemical imprinted sensor for determination of ketamine based on modified polytyramine/sol-gel/f-MWCNTs@AuNPs nanocomposite/pencil graphite electrode, Sens. Actuators B Chem. 259 (2018) 133–141, https://doi.org/10.1016/J.SNB.2017.12.062.
[52] J. Zhou, Y. Xu, L. Wang, J. Liu, Y. Li, B. Ye, Electrochemical behavior and voltammetric determination of ketamine at pulse plating gold film modified platinum electrode, J. Chin. Chem. Soc. 59 (2012) 879–883, https://doi.org/10.1002/JCCS.201100659.